Form follows function — how PufX increases the efficiency of the light-harvesting complexes of *Rhodobacter sphaeroides*

Tihamér Geyer[†]

Zentrum für Bioinformatik, Universität des Saarlandes,
D–66041 Saarbrücken, Germany

Feb. 9, 2007

Abstract

Some species of purple bacteria as, e.g., *Rhodobacter sphaeroides* contain the protein PufX. Concurrently, the light harvesting complexes 1 (LH1) form dimers of open rings. In mutants without PufX, the LH1s are closed rings and photosynthesis breaks down, because the ubiquinone exchange at the reaction center is blocked. Thus, PufX is regarded essential for quinone exchange.

In contrast to this view, which implicitly treats the LH1s as obstacles to photosynthesis, we propose that the primary purpose of PufX is to improve the efficiency of light harvesting by inducing the LH1 dimerization. Calculations with a dipole model, which compare the photosynthetic efficiency of various configurations of monomeric and dimeric core complexes, show that the dimer can absorb photons directly into the RC about 30% more efficient, when related to the number of bacteriochlorophylls, but that the performance of the more sophisticated dimeric LH1 antenna degrades faster with structural perturbations. The calculations predict an optimal orientation of the reaction centers relative to the LH1 dimer, which agrees well with the experimentally found configuration.

For the increased required rigidity of the dimer additional modifications of the LH1 subunits are necessary, which would lead to the observed ubiquinone blockage, when PufX is missing.

Keywords: purple bacteria, photosynthesis, absorption spectrum, efficiency, dimerization

[†]Corresponding author. Address: Zentrum für Bioinformatik, Universität des Saarlandes, Geb. C7.1, Postfach 151150, D–66041 Saarbrücken, Germany
Email: tihamer.geyer@bioinformatik.uni-saarland.de

1 Introduction

Purple bacteria as, e.g., *Rhodobacter (Rb.) sphaeroides* can live on photosynthesis. In this conversion of light into chemical energy, four transmembrane proteins and two electron carriers are involved. It is initiated by photons, which are absorbed in the bacteriochlorophylls (Bchls) of the light harvesting complexes. Their energy is passed on to the special pair Bchls of the RCs. From there, an excited elctron is translocated through the RC onto a bound ubiquinone. Loaded with a second electron and two protons, the reduced quinone unbinds from the RC and delivers its freight to the cytochrome bc_1 complex. From there, the electrons are returned to the RC by two cytochrome c_2 and the protons are released to the periplasm. The resulting proton gradient across the membrane is used by the F_0-F_1-ATP synthase to synthesize ATP. For more details see e.g., (1, 2).

As can be seen on recent atomic force microscopy (AFM) and cryo electron microscopy (EM) images, the photosynthetic membranes of purple bacteria are crowded with the ring shaped LH1s with their embedded RCs and with the auxilliary LH2 (3, 4, 5, 6). In most purple bacteria, the primary LH1 form closed rings of 16 dimeric subunits (7). Each of the subunits consists of two transmembrane helices and two bacteriochlorophylls (Bchl), which are the functionally active parts of the LHCs. In the center of each LH1 ring sits an RC. This assembly of an LH1 with its embedded RC is called a core complex (8). The smaller LH2 are rings of eight or nine subunits only, depending on the species (5, 9).

In some species as, e.g., *Rb. sphaeroides* or *Rb. capsulatus*, an additional small protein PufX is present and the core complexes are dimers of two RCs and two incomplete LH1s of 12 to 13 subunits, each (3, 6, 10, 11, 12). PufX lacking mutants of *Rb. sphaeroides* have closed monomeric LH1 rings and are not able to live on photosynthesis. This deficiency, as shown experimentally, stems from the closed LH1 rings, which slow down the quinone exchange at the RCs to a crawl, such that the RCs are effectively shut off (13, 14). Mutants, where the LH1s are missing, do not require PufX for photosynthetic growth (15). Thus, the current hypothesis about the purpose of PufX is that it opens up the LH1 ring to allow the quinones to access the RC. This hypothesis is confirmed by the latest EM images of the LH1/RC dimers, where the RCs are oriented such that the gap in the LH1 structure is in front of the quinone binding pockets of the RCs (16).

However, this hypothesis about the purpose of PufX does not explain, why most other species of purple bacteria happily live on photosynthesis without PufX and with closed LH1 rings. But there is also a conceptual difficulty with this hypothesis: by making PufX responsible for opening the LH1 for quinone access, the LH1 are implicitly seen as obstacles to efficient photosynthesis, not as an integral and important part of it. The function of the LHCs is to capture photons, they are the antennae of the RCs. The central objective for them is, consequently, to achieve a maximal absorption cross section for photons with a given limited number of Bchls and also to feed the captured photons into the RCs with the least possible loss. We therefore put forth a different hypothesis and propose that the primary purpose of PufX — together with some associated modifications — is to increase the absorption efficiency of the core complexes by inducing their dimerization. Then, allowing for a direct access of the quinones to the RCs becomes necessary because of these modifications to the then open LH1s.

To support our hypothesis, we first present calculations of the absorption properties of

LH1/RC core complexes, which compare the monomeric type without PufX to the dimeric PufX$^+$ configuration. These calculations, which are based on a simple dipole model of the Bchl arrays (17), show that the dimeric configuration can absorb photons directly into the RC at least as good as the monomer, though it has less Bchls. We also find that for this the dimer has to be structurally more rigid. The same advantage is found for monomeric core complexes with an open LH1 ring, a setup, which is found in *Rhodopseudomonas* (*Rps.*) *palustris* (21). From these findings and from recent experimental results, we then argue that the observed blocking of the quinone access to the RCs in PufX$^-$ mutants is a consequence of the increased rigidity of the core complexes from these bacteria, a rigidity, which is necessary to stabilize the dimeric LH1s.

In this publication, which focuses on the differences between the monomeric and the dimeric LH1s, we do not consider the auxilliary LH2s because (i) they are not affected by the presence or absence of PufX and (ii) because their coupling to the core complexes is indirect and relatively slow. In the big picture, their contribution to photosynthesis is to the also neglected non-resonant energy transfer from the LH1s to the RCs.

2 Methods

2.1 Dipole model of the core complex

The calculations of the absorption properties of the different core complex configurations are based on a dipole model introduced by Hu *et al.* (17, 18) (also see (19, 20)). There, the positions and orientations of the RC Bchl dipoles had been determined from the crystal structure (9), while the dipoles of the monomeric LH1 ring were derived from a reconstruction.

Our objective was to compare different core complex configurations from the same species. These are different on a large scale, but can be expected to have the same local environment of the Bchls and the same next neighbor distances. Thus, the same parameters were used for all configurations.

The Bchl positions in the dimeric LH1 were determined by visually fitting two three-quarter rings of the LH1 monomer symmetrically into an EM map of the LH1 dimer. The absorption properties are only minimally sensitive to the exact positions and orientations of the two dimer halves. The two RCs of the dimeric core complex were placed symmetrically into the respective centers of the two halves of the LH1 dimer. For the calculations, the rotation angle of the RCs with respect to their initial orientation, Φ_{RC}, was treated as a free parameter.

The open monomeric core complexes were constructed from the closed monomer by removing adjacent LH1 Bchl dipoles. Here again, the orientation of the RC with respect to the LH1 remainder was treated as a free parameter. The shape of the initially circular LH1 ring was not distorted, also the RC was always put at the center of the original circle, even though the open rings found in *Rps. palustris* have an unsymmetric elliptical shape.

Arrays were built from the closed monomeric and the dimeric core complexes and placed onto a spherical vesicle of 50 nm diameter. According to AFM images (3) and our reconstruction of a chromatophore vesicle (24), the dimers were assembled as a chain with each unit rotated by 10 degrees clockwise. To fit onto the vesicle, the dimers had to be bent at their joint
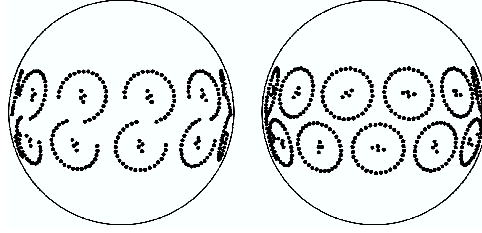
Figure 1: Sketch of the arrays of core complexes on a vesicle of 50 nm diameter that were used for our calculations. The dots denote the positions of the Bchls of the 11 Z-shaped dimers (left panel) and of the 24 closed monomers (right panel). In the dimeric setup the RCs are shown in their most efficient orientation, while in the monomeric configuration they are oriented randomly.

by $26°$. The vesicle was large enough for 11 dimeric core complexes with a total of 616 Bchls. For comparison, a similar setup on a vesicle was constructed with monomeric core complexes, too, where 24 monomers with their 864 Bchls were arranged alternatingly in two rows parallel to the equator of the vesicle. Both configurations are shown in figure 1.

2.2   Total absorption cross section and photosynthetic efficiency

The eigenstates $|\Phi_n\rangle = \sum a_{ni}|i\rangle$ of an array of dipoles and their absorption cross sections, determined by their oscillator strengths $|f_n^2|$, were calculated as explained in (17) with a Hamiltonian from all Bchls of the given configuration.

The total absorption cross section of a certain configuration is $\sum f_n^2 = N$ according to the dipole summation rule. It states that no absorption cross section is lost by coupling the N dipoles. Consequently, the total absorption cross section is not a meaningful measure for the efficiency of a given core complex configuration, because it is solely determined by the number of Bchls.

Absorbing light in an LHC is only the very first step of photosynthesis. The absorbed photons then have to be transferred to the special pair Bchls of the RCs in order to trigger a charge separation. Between the absorption and the charge separation, the energy of the photon can be lost due to thermal relaxation. This efficiency degrading loss process becomes the more important, the longer the electronic excitation takes to travel from the Bchls of the LHCs to the special pair of the RC. Consequently, the most lossless transfer would be an absorption of the photon directly into the special pair.

To describe how direct a given state absorbs photons into the special pair, we introduce the photosynthetic cross section σ_n of an eigenstates $|\Phi_n\rangle$ of a given core complex configuration. It is the product of its absorption cross section f_n^2 and of the probability S_n that one of the special pair Bchls is excited in this state. S_n is calculated from the incoherent sum of the weights $|a_{ni}|^2$ of the special pair (SP) Bchls:

$$\sigma_n = f_n^2 \, S_n = f_n^2 \sum_{SP} |a_{ni}|^2 \tag{1}$$

From this state specific absorption into the RC we define the total photosynthetic cross section Σ of a given configuration as $\Sigma = \sum \sigma_n$. Obviously, for Σ there is no summation rule. Different configurations with the same number of Bchls may have different total photosynthetic cross sections. From the two cross sections $\sum f_n^2 = N$ and Σ, the photosynthetic efficiency η is introduced as $\eta = \frac{\Sigma}{N}$. This efficiency can either be interpreted as the fraction of absorbed photons that is directly available to induce a charge separation in the RC, or as the fraction of the Bchls that couples directly to the RC Bchls.

2.3 Thermal disorder

Thermal disorder of the Bchls modifies their positions and orientations and, by this, their site energies and coupling parameters, and finally the photosynthetic cross section. As only direct, instantaneous photon capture into the special pair Bchls is considered, we can assume that the thermal fluctuations are much slower than the actual photon absorption. The resulting quasistatic deformations of the core complex, which consequently also include static spatial deformations, are captured in the effective Hamiltonian model by a random perturbation of the site energies and of the coupling terms.

To investigate the stability of Σ against thermal fluctuations and spatial deformations, the off–diagonal entries of the Hamiltonian that characterize the interactions and the diagonal entries for the site energies were independently multiplied by random numbers drawn from a Gaussian distribution centered around 1 with a relative width of $\Delta E/E$ of up to 12%. The distribution was modified such that the product of all random numbers is 1, i.e., that the fluctuations do not introduce an energy shift. Perturbing only the interactions or the site energies leads to the same behavior of Σ, however, for the same effect the interaction terms had to be perturbed about four times as strong as the site energies. To achieve stable average values for Σ, the calculations were repeated 200 times for every chosen $\Delta E/E$.

3 Results

3.1 Closed monomeric core complexes

The benchmark configuration of the closed monomeric core complex, which is found in most purple bacteria, consists of the 16–unit LH1 ring with two Bchls each, and an embedded RC. In the dipole model, the empty LH1 ring with its essentially circular symmetry has two degenerate states with orthogonal dipole moments, absorbing at a wavelength of 875 nm. These two states, with $f_{2,3}^2 = 15.7$ each, carry most of the total oscillator strength of $\sum f_n^2 = 32$ (17) (All cross sections are given in units of the dipole moment of the S_y transition of a Bchl).

With th RC inside the LH1 ring, the circular symmetry is broken. From one of the two main LH1 states and the RC groundstate two hybrid LH1-RC states emerge with oscillator strengths of $f_2^2 = 13.0$ and $f_4^2 = 5.82$ and energies corresponding to wavelengths of 876 nm and 864 nm, respectively. The other LH1 state remains unchanged, as its dipole moment is perpendicular to the RC dipoles. These three states 2, 3, and 4 together are responsible for 96% of the total absorption cross section. Their respective photosynthetic cross sections, i.e., their cross section
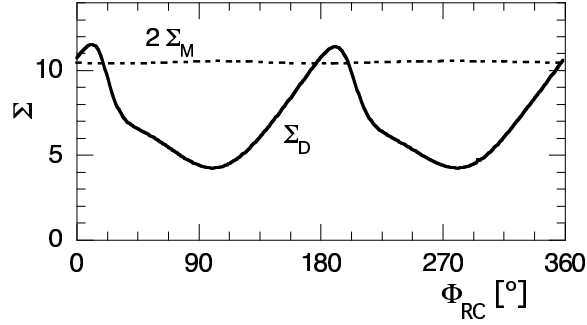
Figure 2: Total photosynthetic cross section $\Sigma_D(\Phi_{RC})$ of the LH1 dimer with its two RCs (solid curve), compared to two times Σ_M of a single RC in a closed monomeric LH1 (broken curve). The angle Φ_{RC} denotes the orientation of the RCs relative to their initial positions. Note that two monomeric core complexes together contain 72 Bchls, while the dimeric core complex only has 56 Bchls.

for absorption directly into the special pair Bchls of the RC, are $\sigma_2 = 0.82$, $\sigma_3 = 8 \times 10^{-5}$, and $\sigma_4 = 4.25$: photosynthesis runs on the LH1/RC hybrid states 2 and 4, while the probility to induce a charge transfer in the RC is negligible in state 3 with its dipole moment orthogonal to the RC dipoles. Summing up all σ_n results in a total photosynthetic cross section of $\Sigma_M = 5.22$ for the closed monomeric core complex and a corresponding efficiency of $\eta_M = 0.145$: effectively one out of every seven of the 36 Bchls contributes *directly* to photosynthesis. The other 85% of the absorbed light have to be handled by higher order transitions between the states, by energy downconversion processes, or they are directly dissipated as heat.

3.2 Open dimeric core complexes

While in the dipole model the closed LH1 ring has a circular symmetry, the Z–shaped LH1 dimer only has a twofold symmetry axis and its eigenstates are not degenerate. Its absorption spectrum is dominated by the three low lying states 1, 3, and 5, which absorb at 882, 875, and 866 nm, respectively. Their oscillator strengths are $f_1^2 = 10.0$, $f_3^2 = 27.6$, and $f_5^2 = 6.97$, i.e., together they account for 94% of the total absorption cross section. Interestingly, state 5 has an energy very close to the RC groundstate at 865 nm. It can be expected that this state will couple very well to the RCs.

With the RCs inserted into the LH1 dimer, the energies and oscillator strengths, i.e., the absorption spectrum of the LH1/RC combination states, vary only little with the rotation angle Φ_{RC} of the RCs. However, the photosynthetic efficiency, which is determined by the coupling between the LH1 and the RCs, is very sensitive to Φ_{RC}.

Figure 2 compares $\Sigma_D(\Phi_{RC})$ of the dimeric core complex to twice Σ_M of the monomer. As expected from the circular symmetry of the monomer, Σ_M is constant for all orientations of the RC, while for the dimer there are two pronounced maxima spaced 180° apart. At these maxima, the dimeric core complex with its 56 Bchls can absorb photons directly into the RCs with a photosynthetic cross section of $\Sigma_D = 11.5$. Two independent monomers with their 72 Bchls, present a cross section of only $2\Sigma_M = 10.4$. Consequently, for optimal orientation of the
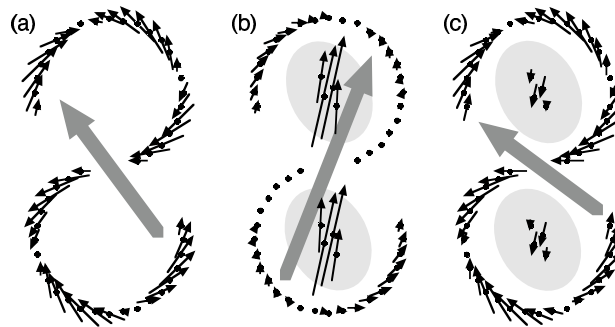
Figure 3: Sketch of state 5 of the empty LH1 dimer (panel (a)) and of states 5 and 7 of the dimeric core complex with optimally oriented RCs (panels (b) and (c), respectively). These two states are formed from state 5 of the empty dimer and the RC groundstate. State 5 (panel (b)) is the photosynthetically active state, while in state 7 the coupling between LH1 and RCs is negligible. The dots denote the positions of the dipoles in the membrane plane as seen from the cytoplasmic side, the black arrows give the direction of each Bchl dipole and, via their length, their weights $|a_{ni}|^2$ in the respective state. The total dipole moment of the states is denoted by the gray arrows. The position of the RCs, as indicated by the shaded regions, compares well to the reconstruction by Qian *et al.* (16).

RCs, the efficiency of the dimer of $\eta_D = 0.21$ is about 30% higher than that of the monomer of $\eta_M = 0.15$.

The orientation of the RCs and the individual weights $|a_{ni}|^2$ of the dipoles at the optimal orientation of the RCs are sketched in figure 3 for the two most important states. For comparison, panel (a) shows state 5 of the empty dimer, which absorbs at 866 nm. This state couples to the RC groundstate to form the two states 5 and 7 of the dimeric core complex shown in panels (b) and (c). Both states absorb at about 865 nm, but with photosynthetic cross sections of $\sigma_5 = 9.66$ and $\sigma_7 = 0.2$, respectively, i.e, they form one "photosynthetic" and one "anti–photosynthetic" state.

Interestingly, the orientation of the RCs, as indicated in figure 3, corresponds well to the orientation found in the reconstruction by Qian *et al.* (16). Thus, not only the access for the quinones to and from the RCs is possible through the gap in the LH1, but it is also the configuration, in which the coupling between the LH1 and the special pair Bchls of the RCs is most efficient.

One can see from figure 2 that for bacteria with dimeric core complexes it makes a huge difference, whether all RCs are oriented optimally with respect to their LH1 antenna or whether they are oriented randomly. Thus, in PufX containing species there should be some mechanism to lock the orientation of the RCs inside the LH1, a feature which is not required with the symmetric closed LH1 monomers.
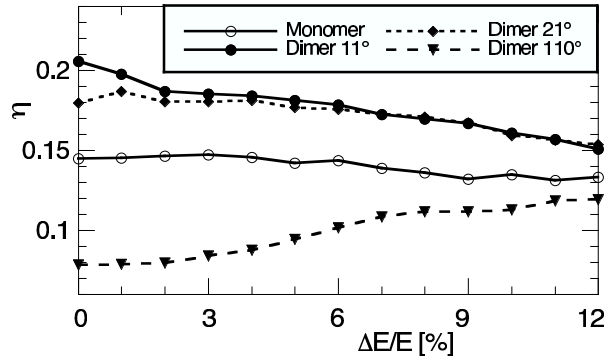
Figure 4: Photosynthetic efficiency η vs. thermal perturbation, indicated by the relative width of the distribution of the interaction strengths, $\Delta E/E$, for the monomer and the dimer with three different orientations of the RCs (cf. figure 2). The lines connecting the data points serve as a guide to the eye. For further explanations see text.

3.3 Thermal disorder and structural stability

Next we have to investigate the performance of the core complexes under more realistic conditions than in the fixed setup of zero temperature used above.

Figure 4 shows, how the photosynthetic efficiency η decreases with increasing thermal disorder. For this figure, only the interaction terms were perturbed. The efficiency of the dimeric core complex is shown for three orientations of the RCs (cf. figure 2): for the optimal orientation of $\Phi_{RC} = 11°$, for slightly misaligned RCs ($\Phi_{RC} = 21°$), where the dimer has about the same Σ as two monomers, and for the most unfavorable configuration of $\Phi_{RC} = 110°$.

The efficiency of the monomer is only slightly affected by the disorder, it decreases from 0.15 without disorder to about 0.13 at $\Delta E/E = 12\%$. In the dimer, the advantage with optimally aligned RCs over a core complex with slightly misaligned RCs vanishes at already small perturbations, but at all perturbations the dimer is more efficient than the monomer, as long as the RCs point into about the right direction. For even stronger disorder, the efficiency of all configurations, i.e, of the monomer and of the dimer with any orientation of the RCs, tends to the same value of around 0.13.

Obviously, the monomer with its closed LH1 ring is more stable against disorder than the open ring dimer. In other words, the closed LH1 can easily be deformed away from its circular shape or the RC can move inside the ring without degrading its antenna function noticeably. The dimer, however, which is a more sophisticated and optimized structure, has to be kept in shape in order to take advantage of its better performance.

Experimental observations show, as we will explain later, that the bacteria go the most obvious way to stabilize their dimeric LH1 antennae via a strong association bweteenm the flexible LH1 chain and the globular RC.
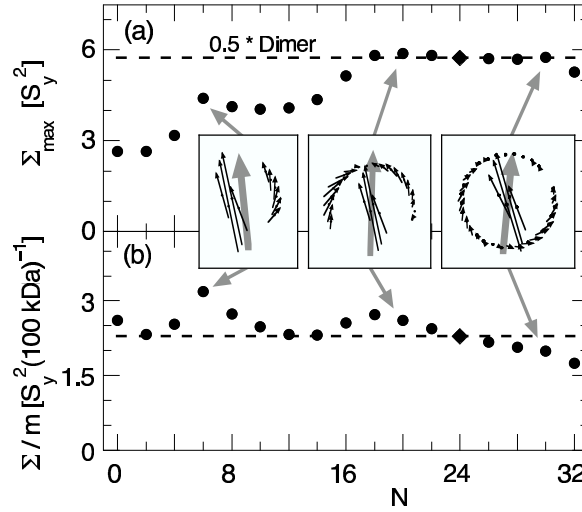
Figure 5: Photosynthetic cross section Σ for monomeric core complexes with partial LH1 rings with various numbers of Bchls, N: (a) Σ for optimal orientation of the RC in the respective partial ring. (b) Σ normalized to the total mass of an RC plus the partial LH1 ring. The RC contributes a mass of 101 kDa and the complete LH1 ring of 200 kDa (9). Half of the respective values from the dimer are indicated in both panels by the diamonds and the horizontal broken lines. The insets sketch the main photosynthetically active states at N=6, 20, and 30 analogous to figure 3.

3.4 Open monomeric core complexes

In the model, the spectrum of the empty closed monomeric LH1 has one absorption line at 875 nm from two degenerate states (see above). When a part of the LH1 ring is removed, the circular symmetry is broken. Together with the now also nonsymmetric groundstate, the open LH1 ring has three main absorbing states, the energies of which increase with decreasing number of Bchls (data not shown). At $N = 24$ Bchls, the highest of these three levels comes in resonance with the RC groundstate at 865 nm.

In the open monomer, the orientation of the RC again determines Σ. Panel (a) of figure 5 plots the maximal Σ at optimal orientation of the RC for core complexes from $N = 32$, i.e., for the closed monomer, down to $N = 0$, which is an RC without any LH1 chain. For comparison, half of the cross section of the dimer is also given. One can discern three regimes: any configuration in the range $18 \leq N \leq 30$, which is between a bit more than a half ring and a nearly complete ring, has essentially the same Σ, though for every N the RC has a different optimal orientation with respect to the symmetry axis of the partial ring. This constant cross section is even higher than with the closed LH1 ring. The other two regimes are the ranges $6 \leq N \leq 14$ and $N \leq 4$, i.e., from a quarter to a half ring, and the RC sided by just a small part of the LH1. The reason for this behavior is that in each of these regimes only a part of the LH1 chain couples directly to the special pair Bchls of the RC. When the RC is aligned correctly, these Bchls that do not contribute to the photosynthetically active states, can be removed without degrading the performance.
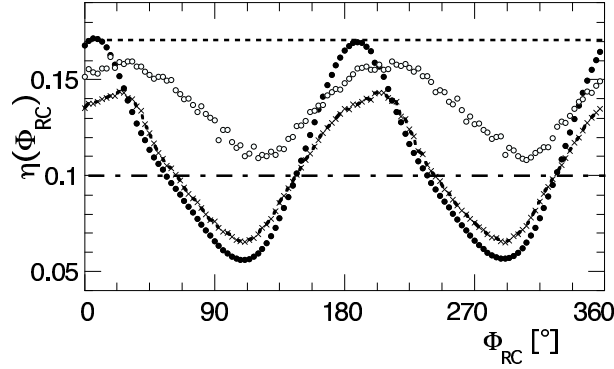
Figure 6: Photosynthetic efficiency η of an array of eleven dimeric core complexes on a vesicle vs. Φ_{RC} for different thermal fluctuations of the interactions of $\Delta E/E = 0$ (solid dots), 1% (crosses), and 8% (open dots). The broken lines at $\eta = 0.17$ and at $\eta = 0.1$ indicate the efficiencies of a single thermally perturbed dimeric core complex (cf. figure 4) and of an array of 24 monomeric core complexes with random orientations of their RCs, respectively. The three-dimensional geometries of the arrays are shown in figure 1.

A different kind of efficiency is plotted in panel (b) of figure 5. Here Σ is not normalized to the number of Bchls, but to the total mass of the core complex. According to (9), the RC has a mass of 101 kDa, while a complete LH1 ring weighs 200 kDa. With respect to the total mass, the core complex with the closed LH1 is the most inefficient configuration, while with any partial LH1 the bacterium has to produce less material for the same yield from direct photon absorption into the RC — if the RC is oriented correctly.

Here again, to make use of the more sophisticated antenna, the orientation of the RC has to be fixed relative to the LH1 and the LH1 has to be stabilized.

3.5 Arrays of core complexes on a vesicle

In a real bacterium there are many core complexes, sitting close together. We therefore have to look at the efficiency of multiple coupled core complexes.

In the array of dimeric core complexes on a vesicle (see figure 1), without any perturbation the most efficient Φ_{RC} is the same as for one independent dimer and Σ follows a similar curve, see figure 6. However, on the vesicle the maximal η is reduced from 0.21 to 0.17. When this highly symmetric model array is perturbed, the behavior is different from that of the isolated core complex. There, the efficiency degraded monotonically with increasing fluctuations. In the array, however, η strongly decreases even with very small perturbations of the interactions of $\Delta E/E \leq 1\%$, only to increase again with increasing $\Delta E/E$. For strong perturbations, the efficiency of the array on the vesicle comes close to that of an equally perturbed isolated dimer, which is indicated in figure 6 by the broken line at $\eta = 0.17$.

This behavior can be understood by comparing the eigenstates of the unperturbed to these of the perturbed system. Two representative states are sketched in figure 7, one without and one with fluctuations. Without fluctuations (panel (a)), the states are highly symmetric. With
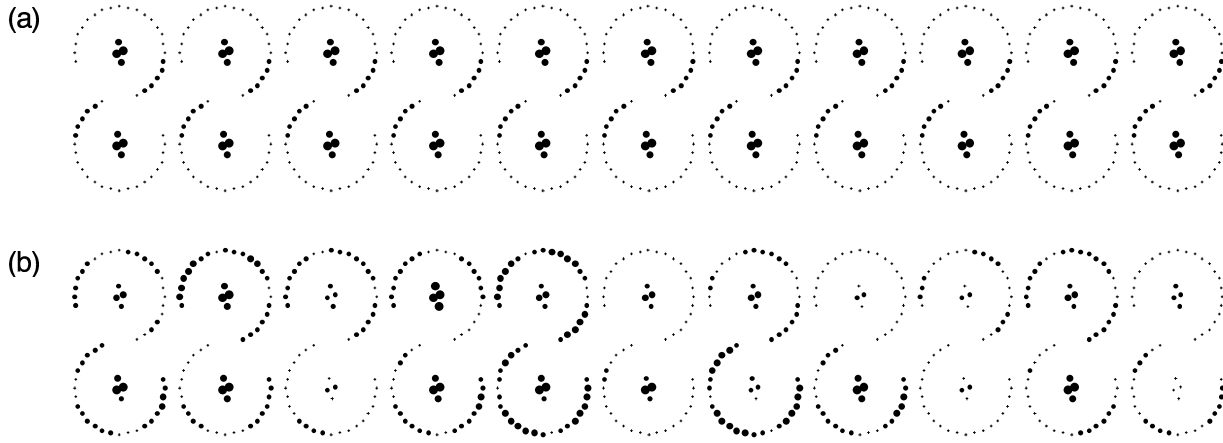
(a)

(b)

Figure 7: Two eigenstates of an array of eleven dimeric core complexes on a vesicle, unrolled into the paper plane (cf. figure 1). The contributions of the individual dipoles, $|a_{ni}|^2$, are indicated by the size of the dots. $\Phi_{RC} = 25°$ for both states. The upper panel (a) shows the main photosynthetically effective state of the unperturbed array with its perfect symmetry. Panel (b) shows a typical photosynthetically effective state at a thermal perturbation of the interactions of $\Delta E/E = 1\%$ (cf. figure 6), which is localized over a few core complexes.

fluctuations (panel (b)), the long range order breaks down and the states become localized over three to five core complexes. Seemingly, the symmetry of the unperturbed array, which is reflected in the eigenstates, only allows for states with a smaller efficiency than possible in an isolated dimer. The symmetry breaking due to the thermal fluctuations relaxes this constraint, and with a stronger perturbation the more efficient localized states lead to the observed increase of the overall efficiency. *In vivo*, the array of core complex dimers on a vesicle will never be perfectly symmetric, as the vesicles are not rigid spheres. Consequently, *in vivo* no strict efficiency degrading long range order will develop and the fluctuations limit the coupling between the core complexes to their respective neighbours, which is good from the perspective of overall efficiency.

Stochastic simulations showed that when a few core complexes are coupled, at intermediate light intensities their yield is increased by some 20%, because the larger combined antenna reduces the statistical fluctuations in the photon supply for each of the involved RCs (22). This might explain, why it is advantageous for the bacteria to closely pack the dimeric core complexes onto chromatophores, even when this slightly reduces the efficiency of absorption directly into the RCs.

As the monomeric core complexes are round and thus have no preferred orientation of the RCs, a random distribution of Φ_{RC} was used when placing the monomers onto the vesicle. Then, the efficiency of the array of $\eta = 0.1$ is much smaller than for isolated core complexes and essentially unaffected by the perturbations. This means that the random orientation of the RCs already introduced more disorder than the thermal fluctuations used here. Also one can conclude that monomeric core complexes are better not packed onto small vesicles, but spread out onto flat membranes, so that they do not disturb each other.

Interestingly, up to now chromatophore vesicles were only found in PufX expressing bacteria with dimeric core complexes, but not in those, where the wild type has monomeric core complexes.

4   Summary and conclusions

Comparing the calculated photosynthetic cross sections and efficiencies of the various configurations of core complexes — the monomer, the dimer, the open monomer, and the two arrays on a vesicle built from monomers and dimers — the following overall picture emerges: without (thermal) perturbation and when the RC is oriented optimally, the photosynthetic efficiency of the dimeric core complex is about 30% higher than that of the monomer. The orientation of the RCs for maximal efficiency determined from the calculations, nicely corresponds to their experimentally determined orientation (16). The open monomer is also more efficient than the closed monomer and here, too, the orientation of the RC for maximal efficiency reproduces the experimentally found orientation in *Rps. palustris* (21). When the photosynthetic cross section is related to the total protein mass of the RC plus the partial LH1 ring, then any open configuration is more efficient than the closed monomer. However, the closed monomeric core complex is the most prominent form in purple bacteria.

With thermal fluctuations, the dimer remains more efficient than the monomer, but with a smaller advantage over the monomer. Also it is more sensitive to these perturbations. The thermal fluctuations were modelled as quasistatic, i.e., as much slower than the photon absorption event itself. Consequently, the closed monomer is also much less sensitive to static deformations of the LH1 ring or to a displacement of the RC away from its optimal position. Thus, the monomer is the more flexible but less efficient configuration, while the more efficient dimer has stronger requirements with regard to structural stability.

The same trend — that the dimer is more efficient, but easier perturbed — is found again, when the core complexes are put onto a typical vesicle. Interestingly, for both the monomer and the dimer, their efficiencies are smaller, when multiple identical core complexes are coupled symmetrically. In this scenario, photosynthesis benefits from the fluctuations, as they destroy the long range order on the vesicle and lead to more efficient localized eigenstates.

Actually, there is a handful of experimental observations that fit nicely with these findings: (i) AFM images of monomeric LH1 rings without an RC showed that the LH1 rings themselves are quite flexible and can easily be deformed (23). (ii) When dimeric core complexes from *Rb. sphaeroides* were reconstituted into planar membranes, a quasicrystalline corrugated long range pattern developed, which is best explained with rigid bent core complexes (12, 24). (iii) Dynamic experiments by, e.g., Barz *et al.* showed that a mutation of *Rb. sphaeroides*, where only the expression of PufX is suppressed without further modification of the LH1, so strongly slows down the diffusion of the quinones to and from the RC, that this PufX$^-$ mutant can not live on photosynthesis any more. However, its photosynthetic competence is partly restored, when the α or β subunits of the LH1 are modified, too (13, 14). (iv) For *Rps. rubrum*, a species without PufX, a recent calculation estimated that a quinone molecule can pass the LH1 ring within about one millisecond, which is fast enough to not impede photosynthesis (25). (v) In the latest high resolution EM images of the dimeric core complex from *Rb. sphaeroides*, two

tentative positions of PufX were identified. It either sits at the joint between the two LH1 halves or between the open ends of the LH1 chains and the RCs (16).

From our calculations and these observations, we put forth the hypothesis, that in these bacteria that express PufX an additional modification of the LH1 chain leads to a strong association between the LH1 and the RC. This would explain, why the dimeric core complexes are rigid, even if the LH1 itself is floppy. In PufX$^+$ species the LH1 chain would stick to the nearly globular RC and thus be stabilized, while in species without PufX in the wildtype the RC can float inside the easily deformed, but closed LH1. Loosely placed inside the closed monomeric LH1 ring, the RC will rotate, but this, too, has no effect on its function. Actually, when the LH1 is easily deformed and there were no association between RC and LH1, the RC would diffuse out of an open LH1. Thus, for the core complex to be stable with an open LH1, these two have to stick together rather strongly.

With regard to the orientation of the RC, it is interesting that Qian *et al.* (16) identified a putative position of the PufX between the open ends of the LH1 ring and the long side of the RC. At this position, PufX could fix the open end of the LH1 chain to the RC and also lock the orientation of the RC with respect to the gap in the LH1 chain. A similar explanation would apply to the position of the PufX homolog found in *Rps. palustris*, which sits between one end of the open monomeric LH1 and the long side of the RC (21).

From the experiments of Barz *et al.* (13, 14) it became clear that PufX is required for fast quinone exchange at the RC. If in *Rb. sphaeroides* the LH1 sticks tightly to the RC and in its PufX$^-$ mutant the gap in the LH1 is missing, then the quinone binding site is blocked. In the suppressor mutants with the modified LH1 chain, the association between the RCs and the LH1 would be weaker, which would allow the quinones to reach the RCs much faster, partly restoring photosynthetic growth.

Consequently, the gap in the LH1 dimer has a dual function: it is both a part of the design of a more efficient antenna, stabilized by PufX and a strong association between the LH1 and the RCs, and it allows for an even faster exchange of the quinones than in species with a loosely attached, but closed LH1 ring.

References

1. Hu, X., T. Ritz, A. Damjanović, F. Authenrieth, and K. Schulten. 2002. Photosynthetic apparatus of purple bacteria. Q. Rev. Biophys. 35:1–62.

2. Geyer, T., and V. Helms. 2006. Reconstruction of a kinetic model of the chromatophore vesicles from *Rhodobacter sphaeroides*. Biophys. J. 91:927–937.

3. Bahatyrova, S., R. N. Frese, C. A. Siebert, J. D. Olsen, K. O. van der Werf, R. van Grondelle, R. A. Niederman, P. A. Bullough, C. Otto, and C. N. Hunter. 2004. The native architecture of a photosynthetic membrane. Nature. 430:1058–1062.

4. Scheuring, S., J. Busselez, and D. Lévy. 2005. Structure of the Dimeric PufX–containing Core Complex of *Rhodobacter blasticus* by *in Situ* Atomic Force Microscopy. J. Biol. Chem. 280:1426–1431.

5. Scheuring, S., J.–L. Rigaud, and J. N. Sturgis. 2004. Variable LH2 stoichiometry and core clustering in native membranes of *Rhodospirillum photometricum*. EMBO J. 23:4127–4133.

6. Siebert, C. A., P. Qian, D. Fotiadis, A. Engel, C. N. Hunter, and P. A. Bullough. 2004. Molecular architecture of photosynthetic membranes in *Rhodobacter sphaeroides*: the role of PufX. EMBO J. 23:690–700.

7. Jamieson, S. J., P. Wang, P. Qian, J. Y. Kirkland, M. J. Conroy, C. N. Hunter, and P. A. Bullough. 2002. Projection structure of the photosynthetic reaction centre-antenna complex of *Rhodospirillum rubrum* at 8.5 Åresolution. EMBO J. 21:3927–3935.

8. Fotiadis, D., P. Qian, A. Philippsen, P. A. Bullough, A. Engel, and C. N. Hunter. 2004. Structural analysis of the reaction center light-harvesting complex 1 photosynthetic core complex of *Rhodospirillum rubrum* using atomic force microscopy. J. Biol. Chem. 279:2063–2068.

9. Koepke, J., X. Hu, C. Muenke, K. Schulten, and H. Michel. 1996. The crystal structure of the light–harvesting complex II (B800–850) from *Rhodospirillum molischianum*. Structure. 4:581–597.

10. Francia, F., J. Wang, G. Venturoli, B. A. Melandri, W. P. Barz, and D. Oesterhelt. 1999. The Reaction Center–LH1 Antenna Complex of *Rhodobacter sphaeroides* Contains One PufX Molecule Which Is Involved in Dimerization of This Complex. Biochemistry. 38:6834–6845.

11. Jungas, C., J.–L. Ranck, J.–L. Rigaud, P. Joliot, and A. Verméglio. 1999. Supramolecular organization of the photosynthetic apparatus of *Rhodobacter sphaeroides*. EMBO J. 18:534–542.

12. S. Scheuring, F. Francia, J. Busselez, B. A. Melandri, J.-L. Rigaud, and D. Lévy. 2004. Structural role of PufX in the dimerization of the photosynthetic core complex of *Rhodobacter sphaeroides*. J. Biol. Chem. 279:3620–3626.

13. Barz, W. P., F. Francia, G. Venturoli, B. A. Melandri, A. Verméglio, and D. Oesterhelt. 1995. Role of PufX Protein in Photosynthetic Growth of *Rhodobacter sphaeroides*. 1. PufX Is Required for Efficient Light–Driven Electron Transfer and Photophosphorylation under Anaerobic Conditions. Biochem. 34:15235–15247.

14. Barz, W. P., A. Verméglio, F. Francia, G. Venturoli, B. A. Melandri, and D. Oesterhelt. 1995. Role of PufX Protein in Photosynthetic Growth of *Rhodobacter sphaeroides*. 2. PufX Is Required for Efficient Ubiquinone/Ubiquinol Exchange between the Reaction Center Q_b Site and the Cytochrome bc_1 Complex. Biochem. 34:15248–15258.

15. McGlynn, P., C. N. Hunter, and M. R. Jones. 1994. The *Rhodobacter sphaeroides* PufX protein is not required for photosynthetic competence in the absence of a light harvesting system. *FEBS Lett.* **349**, 349–353.

16. Quian, P., C. N. Hunter, and P. A. Bullough. 2005. The 8.5 Å Projection Structure of the Core RC–LH1–PufX Dimer of *Rhodobacter sphaeroides*. J. Mol. Biol. 349:948–960.

17. Hu, X., T. Ritz, A. Damjanović, and K. Schulten. 1997. Pigment organization and transfer of electronic excitation in the photosynthetic unit of purple bacteria. J. Phys. Chem. B. 101:3854–3871.

18. Hu, X., and K. Schulten. 1998. Model for the light harvesting complex I (B875) of *Rhodobacter spaheroides*. Biophys. J. 75:683–694.

19. Cory, M. G., M. C. Zerner, X. Hu, and K. Schulten. 1998. Electronic excitations in aggregates of bacteriochlorophylls. J. Phys. Chem. B. 102:7640–7650.

20. Schröder, M., U. Kleinekathöfer, and M. Schreiber. 2006. Calculation of absorption spectra for light-harvesting systems using non-Markovian approaches as well as modified Redfield theory. J. Chem. Phys. 124:084903.

21. Roszak, A. W., T. D. Howard, J. Southall, A. T. Gardiner, C. J. Law, N. W. Isaacs, and R. J. Cogdell. 2003. Crystal structure of the RC-LH1 core complex from *Rhodopseudomonas palustris*. Science. 302:1969–1972.

22. Geyer, T., F. Lauck, and V. Helms. 2007. Molecular stochastic simulations of chromatophore vesicles from *Rhodobacter sphaeroides*. J. Biotech. in press. doi:10.1016/j.jbiotec.2006.12.018.

23. Bahatyrova, S., R. N. Frese, K. O. van der Werf, C. Otto, C. N. Hunter, and J. D. Olsen. 2004. Flexibility and size heterogeneity of the LH1 light harvesting complex revealed by atomic force microscopy. J. Biol. Chem. 279:21327–21333.

24. Geyer, T., and V. Helms. 2006. A spatial model of the chromatophore vesicles of *Rhodobacter sphaeroides* and the position of the cytochrome bc_1 complex. Biophys. J. 91:921–926.

25. Aird, A., J. Wrachtrup, K. Schulten, and C. Tietz. 2007. Possible pathway for ubiquinone shuttling in *Rhodospirillum rubrum* revealed by molecular dynamics simulation. Biophys. J. 92:23–33.